

# Unconventional Magnetic Correlations in $\text{DyB}_2\text{C}$ and $\text{HoB}_2\text{C}$

J. van Duijn and J. P. Attfield

*Department of Chemistry, University of Cambridge, Lensfield Road, Cambridge CB2 1EW, United Kingdom*

R. Watanuki and K. Suzuki

*Graduate School of Engineering, Yokohama National University, 79-5 Tokiwadai, Hodogaya-ku, Yokohama 240-8501, Japan*

R. K. Heenan

*ISIS Pulsed Neutron & Muon Source, Rutherford Appleton Laboratory, Chilton, Didcot OX11 0QX, United Kingdom*

(Received 31 May 2002; published 25 February 2003)

Layered borocarbides  $\text{RB}_2\text{C}$  ( $R = \text{Dy}$ ,  $\text{Ho}$ , and  $\text{Er}$ ) have been studied by powder neutron diffraction at 2–30 K.  $\text{ErB}_2\text{C}$  has two-sublattice antiferromagnetic order below  $T_N = 16.3$  K, but  $\text{DyB}_2\text{C}$  and  $\text{HoB}_2\text{C}$  show a coexistence of a conventional canted  $\mathbf{k} = (000)$  ferromagnetic structure and unconventional magnetic correlations. The  $\mathbf{k} = (000)$  phase orders at  $T_c = 8.5$  K ( $\text{DyB}_2\text{C}$ ) and 7.1 K ( $\text{HoB}_2\text{C}$ ), but low- $Q$  diffraction peaks from the unconventional correlations appear above  $T_c$  with different critical temperatures for different peaks: at 8, 10.5, and 15.7 K for  $\text{HoB}_2\text{C}$ . This scattering is fitted as diffraction from a Warren-type random magnetic layer lattice and may result from quadrupolar interactions between  $R^{3+}$  spins.

DOI: 10.1103/PhysRevLett.90.087201

PACS numbers: 75.30.-m, 61.12.Ld, 72.25.-b, 75.50.Cc

Layered rare earth borocarbides are of interest for their low temperature electronic and magnetic properties. They are generally metallic and contain layers of planar,  $\pi$ -bonded borocarbide layers sandwiching  $R^{3+}$  cations that have localized  $4f^n$  configurations. The  $\text{RB}_2\text{C}_2$  family was studied extensively following the discovery of antiferroquadrupolar order at  $T_Q = 24.7$  K in  $\text{DyB}_2\text{C}_2$  [1,2].

A variety of magnetic phases including spin density wave structures are found in other  $\text{RB}_2\text{C}_2$  [3–6]. The magnetic properties of the related  $\text{RB}_2\text{C}$  family of borocarbides ( $R = \text{Sc}$ ,  $\text{Y}$ , and  $\text{Tb-Lu}$ ) [7–9] have not been reported. These contain planar  $\text{B}_2\text{C}$  sheets of fused 4- and 7-membered rings, with the  $R$  cations located between the 7-membered rings of successive sheets (Fig. 1). It was originally reported that successive  $\text{B}_2\text{C}$  layers were rotated by  $90^\circ$  giving a tetragonal structure [1–3]; however, a reinvestigation of  $\text{HoB}_2\text{C}$  [10] has shown that the  $\text{B}_2\text{C}$  layers are stacked directly above each other leading to an orthorhombic structure (space group  $Pbam$ ), which may have a slight monoclinic distortion to  $P112/m$  symmetry, although this has not yet been proven. Despite the lowering of symmetry, the  $R$  cation array remains pseudotetragonal. We report here a low temperature neutron powder diffraction study of  $\text{DyB}_2\text{C}$ ,  $\text{HoB}_2\text{C}$ , and  $\text{ErB}_2\text{C}$  which has revealed unconventional magnetic correlations in the first two materials.

Polycrystalline samples of  $\text{RB}_2\text{C}$  ( $R = \text{Dy}$ ,  $\text{Ho}$ ,  $\text{Er}$ ) were prepared by arc melting 7 g pellets of the powdered elements (99.9%  $R$ , submicron 99.999% graphite, and 99.1% boron-11 isotope to minimize neutron absorption) on a water cooled copper hearth in an argon atmosphere. The samples were remelted several times to improve homogeneity. Neutron scattering experiments between 4

and 30 K were performed on diffractometer D1B at the Institute Laue-Langevin, Grenoble, France. The samples were placed in a sealed vanadium can within a He cryostat. An annular sample of  $\text{DyB}_2\text{C}$  was used in view of the large absorption cross section of natural Dy. Diffraction

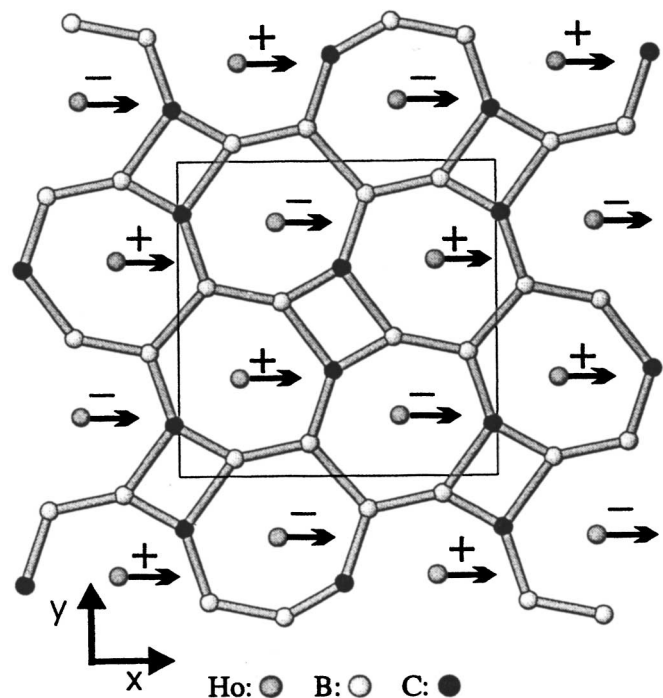


FIG. 1. [001] projection of the  $\text{HoB}_2\text{C}$  structure. The ferromagnetic  $x$  components of the  $\mathbf{k} = (000)$  magnetic structure are shown and the antiferromagnetic  $z$  components are indicated by +, -.

profiles were recorded over  $2^\circ$ – $82^\circ$   $2\theta$  at a neutron wavelength of  $2.52 \text{ \AA}$ , giving a wave vector range of  $Q = 0.1$ – $3.3 \text{ \AA}^{-1}$ . Rietveld analyses were carried out using the FULLPROF program [11]. Additional, time-of-flight neutron spectra of  $\text{HoB}_2\text{C}$  were recorded on the LOQ instrument at the ISIS spallation source, U.K.

The neutron profile of  $\text{ErB}_2\text{C}$  was fitted by the monoclinic  $\text{HoB}_2\text{C}$  structural model [4] [ $a = 6.736(6)$ ,  $b = 6.757(5)$ ,  $c = 3.636(9) \text{ \AA}$ , and  $\gamma = 90.12(8)^\circ$  at  $18.5 \text{ K}$ ]. A single antiferromagnetic ordering transition is observed at  $T_N = 16.3 \text{ K}$ . The magnetic peaks are all indexed by the  $\mathbf{k} = (000)$  propagation vector, and the intensities at  $4 \text{ K}$  were fitted by a collinear, two-sublattice antiferromagnetic model, with Er moments of  $9.06(5) \mu_B$  in the  $c$  direction at  $(\pm 0.31, \pm 0.81, 0.5)$  antiparallel to those at  $(\pm 0.19, \pm 0.31, 0.5)$ .

$\text{HoB}_2\text{C}$  [ $a = 6.760(1)$ ,  $b = 6.761(1)$ ,  $c = 3.6901(2) \text{ \AA}$ , and  $\gamma = 90.16(2)^\circ$  at  $30 \text{ K}$ ] shows an unusual evolution of magnetic neutron scattering at low temperatures (Fig. 2). Between  $16$  and  $8 \text{ K}$ , three peaks appear at low  $Q$ , all with different critical temperatures (Fig. 3). Sharp, resolution-limited peaks occur at  $d = 11.43 \text{ \AA}$  [ $T_c = 15.7(2) \text{ K}$ ] and at  $d = 22.78 \text{ \AA}$  [ $T_c = 10.5(3) \text{ K}$ ], and a broad, asymmetric peak appears at  $d = 35.8 \text{ \AA}$  ( $T_c = 8 \text{ K}$ ). The former two peak intensities follow typical critical behavior below their  $T_c$ 's, with exponents of  $\beta = 0.32(4)$  and  $0.33(7)$ , respectively, whereas the intensity evolution of the broad  $35.8 \text{ \AA}$  peak (Fig. 3) evidences strong critical fluctuations above the  $T_c$ . To verify that the unusual low- $Q$  peaks are elastically scattered and are intrinsic to the sample, additional time-of-flight measurements at  $2$ – $20 \text{ K}$  [Fig. 2(b)] were made on the LOQ spectrometer. The same low- $Q$  peaks are evident in these spectra, with the same temperature variations as above, although the lower instrumental resolution prevents the  $36 \text{ \AA}$  peak from being resolved from small angle scattering of the incident beam.

A conventional magnetic order transition occurs at  $T_c = 7 \text{ K}$  in  $\text{HoB}_2\text{C}$ , with many magnetic diffraction peaks indexed by propagation vector  $\mathbf{k} = (000)$  appearing simultaneously at longer  $Q$ . These magnetic diffraction intensities are fitted by a canted spin model (Fig. 1), in which the  $z$  spin components have the same antiparallel arrangement as those in  $\text{ErB}_2\text{C}$ , but with additional ferromagnetic components of  $2.4(3) \mu_B$  per  $\text{Ho}^{3+}$  present in the  $xy$  plane. The resultant moments are canted by  $56.1(9)^\circ$  from the  $c$  direction and have a magnitude of  $2.94(2) \mu_B$  at  $4 \text{ K}$ . This is considerably less than expected for  $\text{Ho}^{3+}$ , for example, in  $\text{HoB}_2\text{C}_2$  ( $T_c = 5.8 \text{ K}$ ) the ordered  $4 \text{ K}$  moment is  $7.8 \mu_B$  [3]. The temperature variation of the  $(110)$  magnetic intensity (Fig. 3) is fitted with critical exponent  $\beta = 0.36(4)$ .

The low Ho moment in the  $\mathbf{k} = (000)$  magnetic phase and the absence of any structural distortions on cooling indicate that the additional low- $Q$  scattering arising between  $16$  and  $8 \text{ K}$  is due to additional magnetic order [12]. This scattering is not typical of spin wave or other magnetic superstructures which are common in rare earth

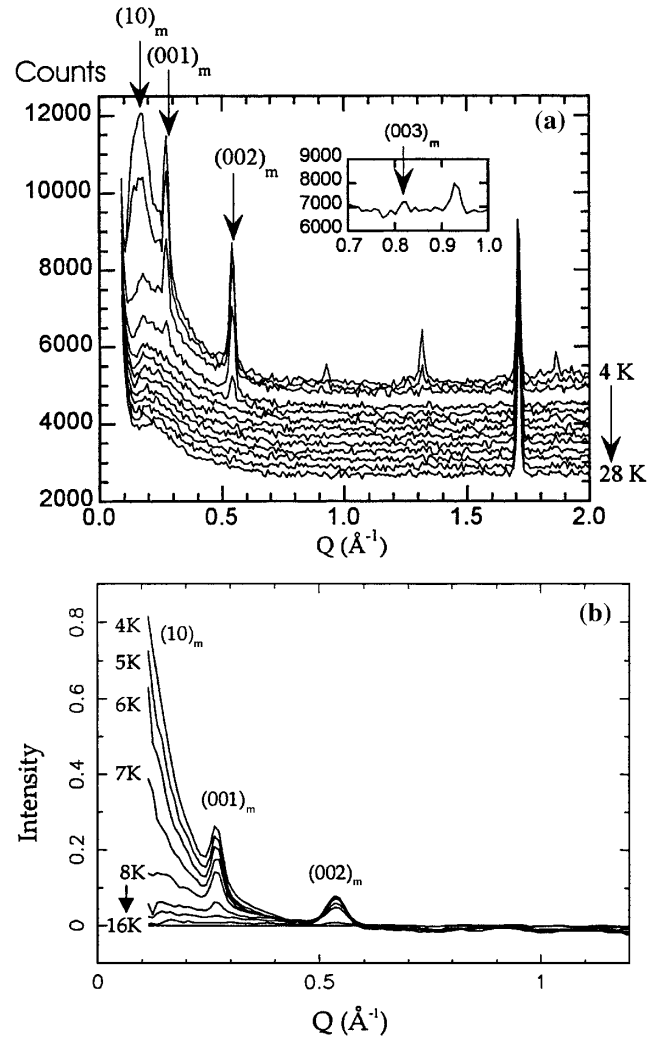


FIG. 2. Neutron diffraction data for  $\text{HoB}_2\text{C}$ . (a) Constant wavelength DIB profiles between  $4$  and  $28 \text{ K}$  in  $2 \text{ K}$  intervals, successively offset by  $200$  counts. Magnetic random layer lattice peaks are indicated and the inset shows the weak  $(003)_m$  peak in a longer scan at  $4 \text{ K}$ . (b) Time-of-flight LOQ data at  $4, 5, 6, 7, 8, 10, 12$ , and  $16 \text{ K}$ ; the  $20 \text{ K}$  spectrum has been subtracted from the spectra shown.

metals and their compounds, but can be described using the random layer lattice theory of Warren [13]. For a lattice of internally ordered layers stacked regularly in the  $c$  direction, but with random layer translations and rotations in the  $ab$  plane, only sharp  $(00l)$  and broad, asymmetric, two-dimensional  $(hk)$  diffraction peaks are observed, and no general  $(hkl)$  reflections result. The low- $Q$  region of the difference between  $4$  and  $30 \text{ K}$  powder neutron diffraction spectra of  $\text{HoB}_2\text{C}$  was fitted by peaks of arbitrary intensity within the Warren model. The  $22.78$  and  $11.43 \text{ \AA}$  peaks were assigned as  $(001)_m$  and  $(002)_m$  (the  $m$  subscript refers to the magnetic random layer lattice throughout) and were fitted using a Gaussian peak shape function. The indexing was corroborated by observation of a very weak  $(003)_m$  peak at  $d = 7.7 \text{ \AA}$  [see Fig. 2(a) inset]. The asymmetric  $35.8 \text{ \AA}$  peak was

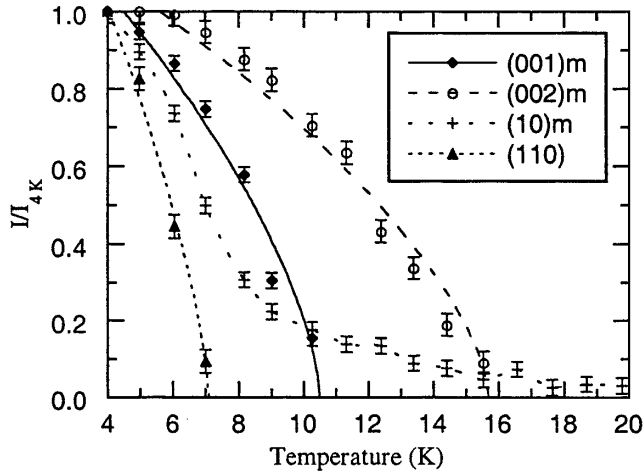


FIG. 3. Thermal evolution of magnetic peak intensities (normalized to 4 K values) for  $\text{HoB}_2\text{C}$ . The  $(001)_m$ ,  $(002)_m$ , and  $\mathbf{k} = (000)$  phase  $(110)$  intensities, shown below their  $T_c$ 's, are fitted as  $I = I_0(1 - T/T_c)^{2\beta}$ . The  $(10)_m$  intensities are shown over the entire temperature range with an empirical curve.

assigned as  $(10)_m$  and was fitted by the Warren function [13]. Residual intensity at  $d \approx 25 \text{ \AA}$  was fitted by a second Warren peak at the tetragonal  $(11)_m$  position. The good overall fit (Fig. 4) shows that the low- $Q$  magnetic scattering features for  $\text{HoB}_2\text{C}$  are consistent with a magnetic random layer lattice, with tetragonal cell parameters  $a_m = 40(1) \text{ \AA}$  and  $c_m = 22.9(1) \text{ \AA}$ . The correlation length in the  $ab$  plane is estimated to be  $90(3) \text{ \AA} \approx 2.3a_m$  from the  $(10)_m$  peak width. The correlation length in the  $c$  direction is  $> 1000 \text{ \AA}$  as the  $(001)_m$  reflection widths are instrumentally limited.

Magnetic susceptibility data for  $\text{HoB}_2\text{C}$  (Fig. 5) show Curie-Weiss behavior at high temperatures and the effective paramagnetic moment of  $10.86\mu_B$  is close to the free ion value of  $10.60\mu_B$  for  $4f^{10} \text{ Ho}^{3+}$ . Divergence of zero-field-cooled (ZFC) and field-cooled (FC) susceptibilities

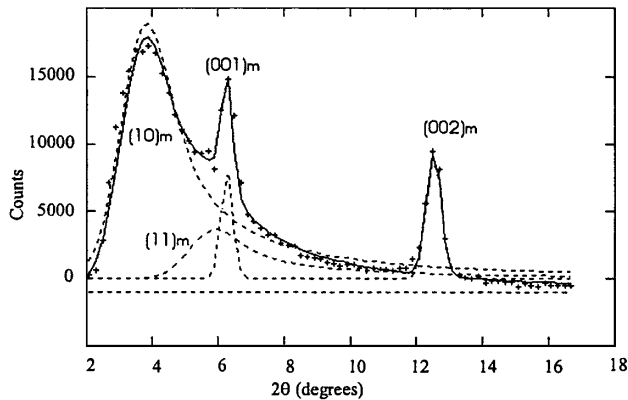


FIG. 4. Fit to the low- $Q$  difference between 4 and 30 K DIB neutron diffraction patterns of  $\text{HoB}_2\text{C}$ . Observed (+) and calculated (full line) profile intensities and individual peak contributions from the magnetic random layer lattice (broken lines) are shown.

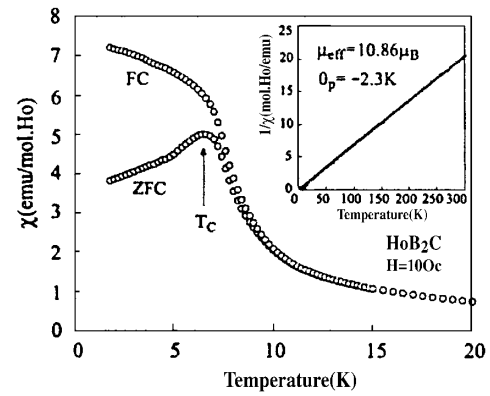


FIG. 5. Low temperature ZFC and FC magnetic susceptibilities of  $\text{HoB}_2\text{C}$ . The inset shows the Curie-Weiss fit to the inverse susceptibility.

is as expected for the 7 K canted ferromagnetic ordering transition. No magnetization anomalies are evident in the 8–16 K region.

$\text{DyB}_2\text{C}$  has cell parameters  $a = 6.764(3)$ ,  $b = 6.763(5)$ ,  $c = 3.704(2) \text{ \AA}$ , and  $\gamma = 90.25(5)^\circ$  at 30 K. The low temperature scattering (Fig. 6) contains similar peaks to those of  $\text{HoB}_2\text{C}$ , although neutron absorption by Dy leads to poorer counting statistics and a relatively intense background feature at  $Q = 0.26 \text{ \AA}^{-1}$ . This overlaps the  $(10)_m$ ,  $(11)_m$ , and  $(001)_m$  peaks, making their temperature variations uncertain. However, the sharp  $(002)_m$  peak at  $d = 11.51 \text{ \AA}$  is clearly resolved and has  $T_c = 21.6 \text{ K}$ . The low  $Q$  difference between scattering at 1.5 and 30 K (Fig. 6 inset) is fitted by the same envelope of asymmetric Warren  $(10)_m$  and  $(11)_m$  peaks and sharp  $(001)_m$  and  $(002)_m$  reflections as for  $\text{HoB}_2\text{C}$  (Fig. 4). The random magnetic layer lattice has tetragonal cell parameters  $a_m = 42(1)$  and  $c_m = 23.0(1) \text{ \AA}$ . The conventional  $\mathbf{k} = (000)$  magnetic phase orders at  $T_c = 8.5 \text{ K}$  and the diffraction

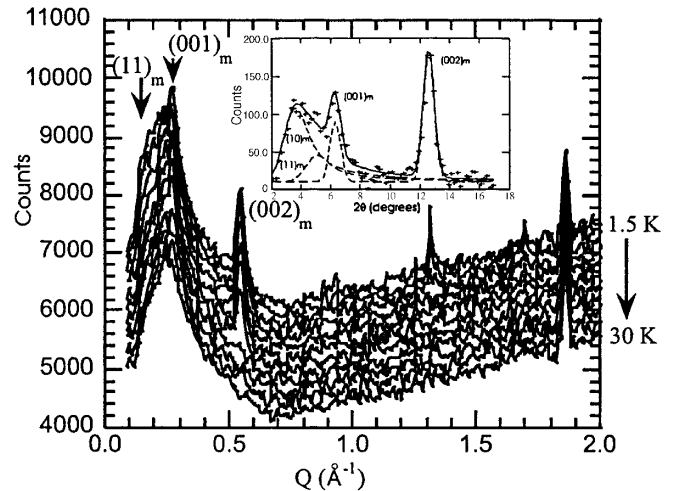


FIG. 6. DIB neutron diffraction patterns for  $\text{DyB}_2\text{C}$  between 1.5 and 30 K. The inset shows the fit to the low- $Q$  difference between 1.5 and 30 K data, as in Fig. 4.

peaks were fitted by the same canted spin model as for  $\text{HoB}_2\text{C}$ . The refined tilt angle from  $c$  is  $47(5)^\circ$  and the ordered Dy moment of  $3.3(3)\mu_B$  at 4 K is much lower than the value of  $8.3\mu_B$  in  $\text{DyB}_2\text{C}_2$  [3]. Magnetization data for  $\text{DyB}_2\text{C}$  are similar to those for  $\text{HoB}_2\text{C}$ ; the paramagnetic effective Dy moment is  $10.63\mu_B$  and the Curie transition is at 8.5 K with divergence of ZFC and FC susceptibilities. Further magnetization and specific heat results for  $\text{HoB}_2\text{C}$  and  $\text{DyB}_2\text{C}$  will be published elsewhere.

The scattering angles and peak shapes of the low- $Q$  magnetic scattering for  $\text{HoB}_2\text{C}$  and  $\text{DyB}_2\text{C}$  are consistent with a Warren-type magnetic random layer lattice, although the crystal structures of the  $\text{RB}_2\text{C}$  samples are ordered in three dimensions. The low- $Q$  scattering is quite different from that of the modulated spin structures that are common in rare earth compounds, e.g., in  $\text{HoB}_2\text{C}_2$  [3,5], which give rise to magnetic satellites of the nuclear Bragg ( $hkl$ ) reflections. The scattering from the  $\text{HoB}_2\text{C}$  and  $\text{DyB}_2\text{C}$  magnetic random layer phases is observed only for  $Q < 0.9 \text{ \AA}^{-1}$ , showing the ordered moments to be small, whereas the  $\mathbf{k} = (000)$  magnetic and nuclear diffraction peaks are found at higher  $Q$ . The lack of any satellite peaks prevents the relative orientation of the nuclear and random layer magnetic cell vectors from being determined in these powder experiments. However, it is likely that the stacking axis of the random magnetic layers  $c_m$  coincides with the  $c$  vector of the pseudotetragonal layered crystal structure. The two periodicities are not commensurate:  $c_m = 6.21(3)c$  for  $\text{HoB}_2\text{C}$ . The same factor of  $\sim 6$  exists between  $a_m$  and the  $a$  or  $b$  nuclear cell parameters.

Another unconventional feature of the low- $Q$  scattering is that the magnetic random layer peaks appear at different temperatures, so they do not necessarily belong to a single magnetic phase. Whether the diffracted intensities are consistent with a single magnetic model from which structure factors could be calculated is not yet clear. The  $(002)_m$  and  $(001)_m$  intensities, and the  $(110)$  peak of the conventional  $\mathbf{k} = (000)$  magnetic phase, all have exponents  $\beta \approx 0.33$  for  $\text{HoB}_2\text{C}$ , which is typical for long range magnetic ordering transitions. The strong critical scattering observed above  $T_c \approx 8 \text{ K}$  is consistent with the two-dimensional nature of the  $(10)_m$  reflection.

The origin and static or dynamic nature of the unconventional magnetic correlations are not yet known, but as  $\text{RB}_2\text{C}_2$  with  $R = \text{Ho}$  and  $\text{Dy}$  both have antiferroquadrupolar ordering transitions ( $T_Q$ ), it seems likely that the unconventional magnetism of the  $\text{RB}_2\text{C}$  analogs is also related to ordering of  $4f^n$  quadrupoles or multipoles. The ordering temperatures for  $\text{DyB}_2\text{C}_2$  are higher than for  $\text{HoB}_2\text{C}_2$  although their magnetic ordering sequences differ;  $\text{DyB}_2\text{C}_2$  has  $T_Q = 24 \text{ K}$ , above the only magnetic phase transition at 18 K, whereas  $\text{HoB}_2\text{C}_2$  has a spin density wave magnetic transition at 5.8 K and a second

magnetic transition at  $T_Q = 5.0 \text{ K}$ . The  $\text{RB}_2\text{C}$  phases are more comparable:  $T_c$  for  $(002)_m = 22 \text{ K}$  for  $\text{DyB}_2\text{C}$  and 16 K for  $\text{HoB}_2\text{C}$ , and the respective  $T_c$ 's for their  $\mathbf{k} = (000)$  phases are 8.5 and 7.1 K.

In conclusion, both  $\text{HoB}_2\text{C}$  and  $\text{DyB}_2\text{C}$  display coexistence of a canted ferromagnetic  $\mathbf{k} = (000)$  spin structure and unconventional magnetic correlations that give rise to low- $Q$  elastic neutron scattering. The scattering angles and shapes of the latter diffraction peaks are consistent with the Warren model of a random layer lattice. However, the peaks appear at different critical temperatures, above that of the  $\mathbf{k} = (000)$  phase. The competing ground states result from complex spin-spin interactions that probably involve quadrupoles or higher multipoles of the  $4f^n$  configurations, coupled to the lattice degrees of freedom, and further measurements and neutron scattering experiments, in particular, from single crystals, will be needed to elucidate this unusual physics.

We acknowledge EPSRC for provision of neutron beam time at ILL and ISIS, EPSRC and ICI Katalco for aid for J.v.D., and the Ministry of Education, Science, Sports and Culture, Japan, for a Grant-in-Aid for Scientific Research on Priority Areas No. 288. We thank Dr. A. Hewat for assistance with neutron data collection and Professor J. B. Forsyth for useful discussions.

- 
- [1] H. Yamauchi *et al.*, J. Phys. Soc. Jpn. **68**, 2057 (1999).
  - [2] K. Hirota, N. Oumi, T. Matsumura, H. Nakao, Y. Murakami, and Y. Endoh, Phys. Rev. Lett. **84**, 2706 (2000).
  - [3] J. van Duijn, J. P. Attfield, and K. Suzuki, Phys. Rev. B **62**, 6410 (2000).
  - [4] K. Ohoyama, T. Onimaru, H. Onodera, H. Yamauchi, and Y. Yamaguchi, J. Phys. Soc. Jpn. **69**, 2623 (2000).
  - [5] K. Ohoyama, H. Yamauchi, A. Tobo, H. Onodera, H. Kadowaki, and Y. Yamaguchi, J. Phys. Soc. Jpn. **69**, 3401 (2000).
  - [6] K. Kaneko, H. Onodera, H. Yamauchi, K. Ohoyama, A. Tobo, and Y. Yamaguchi, J. Phys. Soc. Jpn. **70**, 3112 (2001).
  - [7] J. Bauer and H. Nowotny, Monatshefte für Chemie **102**, 1129 (1971).
  - [8] J. Bauer and J. Debuigne, J. Inorg. Nucl. Chem. **37**, 1473 (1975).
  - [9] J. Bauer, J. Less Common Met. **87**, 45 (1982).
  - [10] J. van Duijn, J. P. Attfield, R. Watanuki, and K. Suzuki, J. Phys. Chem. Solids **62**, 1423 (2001).
  - [11] J. Rodriguez-Carvajal, Physica (Amsterdam) **192B**, 55 (1993).
  - [12] This is corroborated by a preliminary low temperature x-ray diffraction study of the same  $\text{HoB}_2\text{C}$  powder. Data collected at 2 K on instrument ID31 at The European Synchrotron Radiation Facility, Grenoble, France, show no sample scattering peaks in the  $Q = 0.2\text{--}1.2 \text{ \AA}^{-1}$  range.
  - [13] B. E. Warren, Phys. Rev. **59**, 693 (1941).